



UNITED NATIONS
UNIVERSITY

UNU-GTP

Geothermal Training Programme

Orkustofnun, Grensasvegur 9,
IS-108 Reykjavik, Iceland

Reports 2019
Number 9

POWER PLANT AND THERMOECONOMICS MODELLING OF LOW- TO INTERMEDIATE-TEMPERATURE GEOTHERMAL RESOURCE IN MONTELAGO, PHILIPPINES

Jeffrey M. Andal

Department of Energy
Energy Center, Rizal Drive
Bonifacio Global City, Taguig City 1632
PHILIPPINES
andal_jef@yahoo.com.ph

ABSTRACT

The growth of the geothermal industry in the Philippines remains slow despite the initiatives of the government. Based on the study made by the Philippines' Department of Energy, one of the major factors affecting the growth is the high cost of development for low-to-intermediate temperature geothermal resources. To provide a deeper understanding of this cost, we performed power plant modelling and thermoeconomics modelling for a prospective geothermal power plant in Montelago, Philippines. The models in this report were used to determine the following: the optimal power output of the system, the cost of the power plant development, the minimum cost of electricity generation, and exergetic evaluation. The model indicates that the cost of installed power to develop the Montelago geothermal prospect is 3574 USD/kWe and the minimum cost of electricity generation and the break-even point is 6.22 USDcents/kWh and 8.26 USDcents/kWh, respectively. This suggests that further development of the prospect could be economical.

1. INTRODUCTION

Utilization of geothermal energy for power generation plays a very important role in the Philippines. According to the 2018 Power Statistics Report of the Philippines' Department of Energy (DOE, 2019a), geothermal energy provides a total of 10 270 GWh. This is about 10.88% of the total gross generation of the country. So, for every ten lightbulbs, it may be assumed that one lightbulb is powered by geothermal energy. However, despite of this important role in meeting the energy demand of the country, the rate of development of this resource seems to be slowing down. As a response, the Philippines' government continues to promote its utilization.

The country has been exploring geothermal energy for more than fifty years. Its development started on 1967 when the first light bulb using electricity from geothermal, was lit in Tiwi, Albay. Now, the country is the third (3rd) largest power producer in the world using geothermal energy, after the USA and Indonesia, with a total installed capacity of 1918.16 MW (DOE, 2019b). Based on the internal report of the DOE (2019b), since the start of exploitation of geothermal energy for power production in 1977 until 2018, the country has already generated almost 300 000 GWh of electricity using geothermal

providing the country with a clean, reliable, and affordable source of electricity. Based on the DOE's report the geothermal energy development in the Philippines is illustrated in Figure 1.

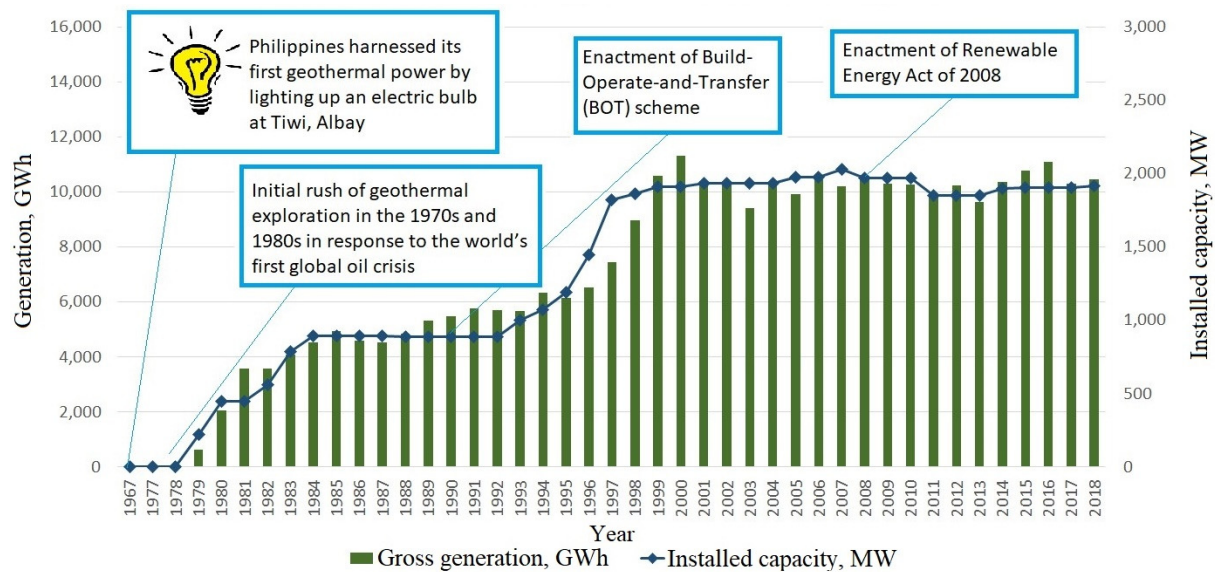


FIGURE 1: Geothermal development in the Philippines

Figure 1 shows that there have been two leaps of development of geothermal energy utilization. These leaps of development have mainly been driven by governmental intervention. The first intervention was when the government addressed the oil-crisis in the mid-1970's by developing indigenous resources such as geothermal energy. This led to the development of Tiwi, Makban, Tongonan, and Palinpinon geothermal power plants. The other spurt of development was in 1990's where the government enacted a law, allowing the Build-Operate-Transfer scheme. This led to the development of the Mt. Apo geothermal field and the expansion of the Tongonan geothermal field (Clemente et al., 2016). Additionally, it can be seen in Figure 1 that the intervention to further develop the utilization of geothermal energy does not stop in 1990's. In 2008, the Philippines' government enacted the Renewable Energy Act, which was intended to promote the development, utilization and commercialization of renewable energy resources in the country. However, despite of commercialization of new power plants and expansion of existing geothermal fields, the development of utilization of geothermal energy remains slow.

According to the DOE (2019b) internal report, the following are the barriers that affects the development of geothermal energy in the Philippines: (1) environmental and socio-cultural concerns in protected areas and ancestral lands; (2) high cost of development for low-to-intermediate temperature and acidic geothermal resources; (3) low-level awareness on non-power applications of geothermal energy; and (4) numerous permits and time-consuming processes to get permits. The identified barriers prompted the government to issue policies and projects to address it. Some of the policies and projects are shown in Table 1 below:

The policies and projects listed aim to assist the investors in tackling the barriers in the development of a geothermal resource. The main barrier is the high cost of development for low-to-intermediate temperature and acidic geothermal resources. While there are few known acidic resources in the Philippines, there are about 428 MW known low-to-intermediate temperature geothermal resources in the country and this number might continue to increase as further studies in several fields are being conducted (DOE, 2019b). Utilizing this low-to-intermediate temperature geothermal resources would be beneficial to the country as these resources are clean and indigenous.

TABLE 1: Policies and projects issued by the Philippines’ government

Policies	Projects
Executive Order No. 30 (Approved June 28, 2017): Creating the Energy Investment Coordinating Council (EICC) in order to streamline the regulatory procedures affecting energy projects.	Detailed assessment of selected low-enthalpy geothermal resources in the Philippines (2010 – 2015).
Republic Act No. 11032 (Approved May 28, 2018): An act promoting Ease of Doing Business and efficient delivery of government services.	Comprehensive resource assessment of Philippine low-enthalpy geothermal areas (2015 – 2017).
Republic Act No. 11234 (Approved March 08, 2019): An act establishing the Energy Virtual one-stop shop for streamlining the permitting process of power generation, transmission, and distribution projects.	Philippine geothermal resource inventory and assessment (ongoing).

Among the areas with low-to-intermediate temperature geothermal resources, one of the most advanced fields in the exploration stage is the Montelago geothermal prospect located in Mindoro Island, Philippines (Figure 2). Thus, this report uses the Montelago geothermal prospect as a case study to provide a better understanding of the cost of development of this type of resource using power plant and thermoeconomics modelling. However, this report will not cover a comparison of development using emerging technologies and this report will not include the barriers that affect the development of a project.

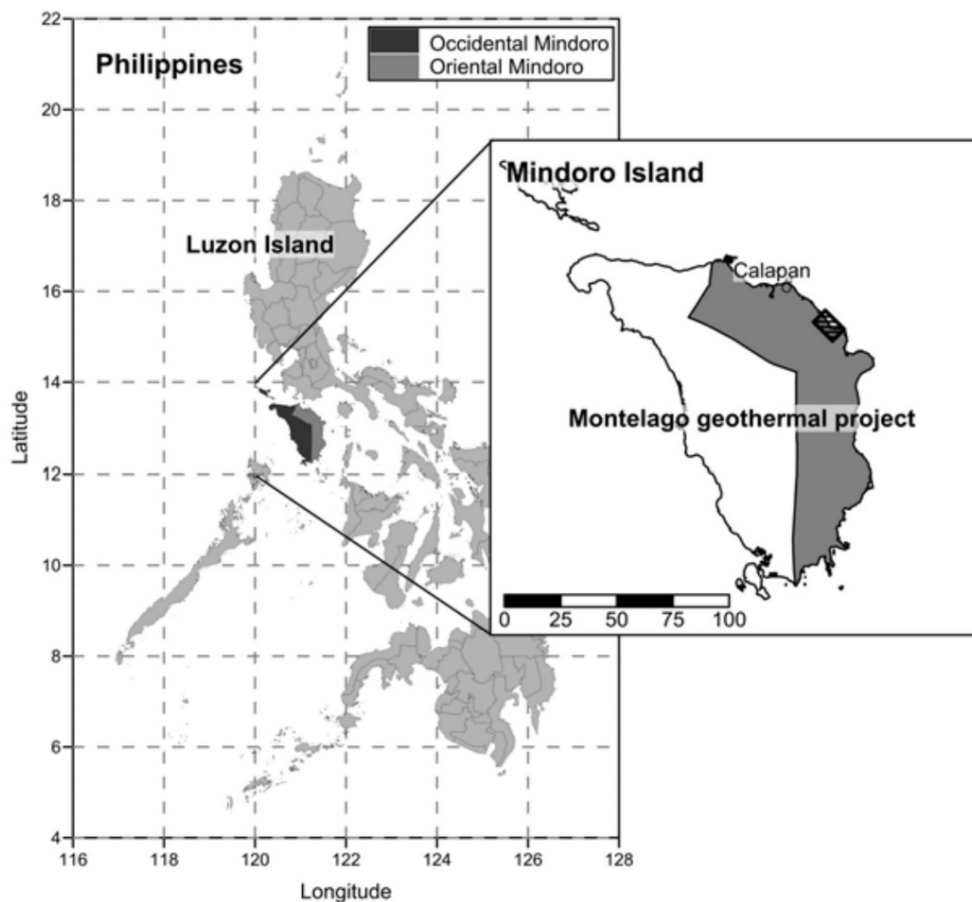


FIGURE 2: Montelago, Philippines (van Leeuwen, 2016)

2. LOW- TO INTERMEDIATE-TEMPERATURE GEOTHERMAL RESOURCES

2.1 Low- to intermediate-temperature fields in the Philippines

A resource with a temperature of less than 150°C is considered a low-temperature resource. These resources can be used for heat pumps or direct use application. Resources with temperatures ranging from 150 to 200°C are moderate or intermediate temperature resources. These intermediate resources can be used for electricity generation, but the wells might require pumping as these wells are not capable of producing large quantities of fluids which are required for large scale electric production (DiPippo, 2016).

According to the DOE's internal report (2019a), it is estimated that the Philippines has a geothermal energy potential of about 4407 MW. As shown on Appendix I., the known estimated potential from the low-to-intermediate temperature geothermal resources is about 428 MW and some fields requires further study to determine their potential.

2.2 Montelago geothermal prospect

2.2.1 Montelago, Mindoro

The Montelago geothermal prospect is in the north western part of Mindoro Island, Philippines between the Naujan lake and Tablas strait. The island of Mindoro is the seventh largest island in the Philippines with a total area of 10 571 km². It has a total population of 1 331 473 (2015). The economy on this island is largely based on agriculture and tourism (Wikipedia.org, 2019).

The prospect has a tropical climate with significant rainfall in Naujan that averages to 2003 mm per year and a short dry season. The average annual temperature in the prospect is 27.3°C (Climate-Data.org, 2019).

2.2.2 Cost of electricity

For 2016, Mindoro island has a total peak demand of more than 64 MW based on the combined total load of the electric cooperatives located in Mindoro (NGCP, 2019). The cost of electricity in Mindoro remains expensive as some part of the island relies on generators fuelled by diesel. According to Ahmed (2019), the true cost of diesel in Mindoro is ranging from 9.60 to 38.47 PHP/kWh or 18 to 74 USDcents/kWh, based on the foreign exchange rate of 1 USD to PHP 52.32 dated 22 August 2019 (XE Corporation, 2019), while the existing subsidized approved generation rate is 11 USDcents/kWh (5.64 PHP/kWh).

2.3 Montelago resource assessment

Several exploration studies had been carried out since 1979 until present. However, these studies made have inconsistencies. To get a good estimate of the potential of the geothermal prospect, this section will describe and adapt information from the recent resource assessment made on the prospect. However, this is not intended to provide a complete review and or to question other studies made on the prospect, but instead is a summary of details that are important for the elaboration of the power plant modelling. Additionally, this report is independent of other previous studies and not meant by any means to criticize the other studies. This report is purely aimed at the evaluation of the resource using modelling.

The prospect has low to moderate elevation and is located between the Naujan lake and Tablas strait. It is bounded by 19 fault lines (Figure 3) and has four eruptive centres, which are Mt. Montelago, Mt. Pungao, Mt. Buloc, and Mt. Matabang Bundok (Asmin et al., 2016).

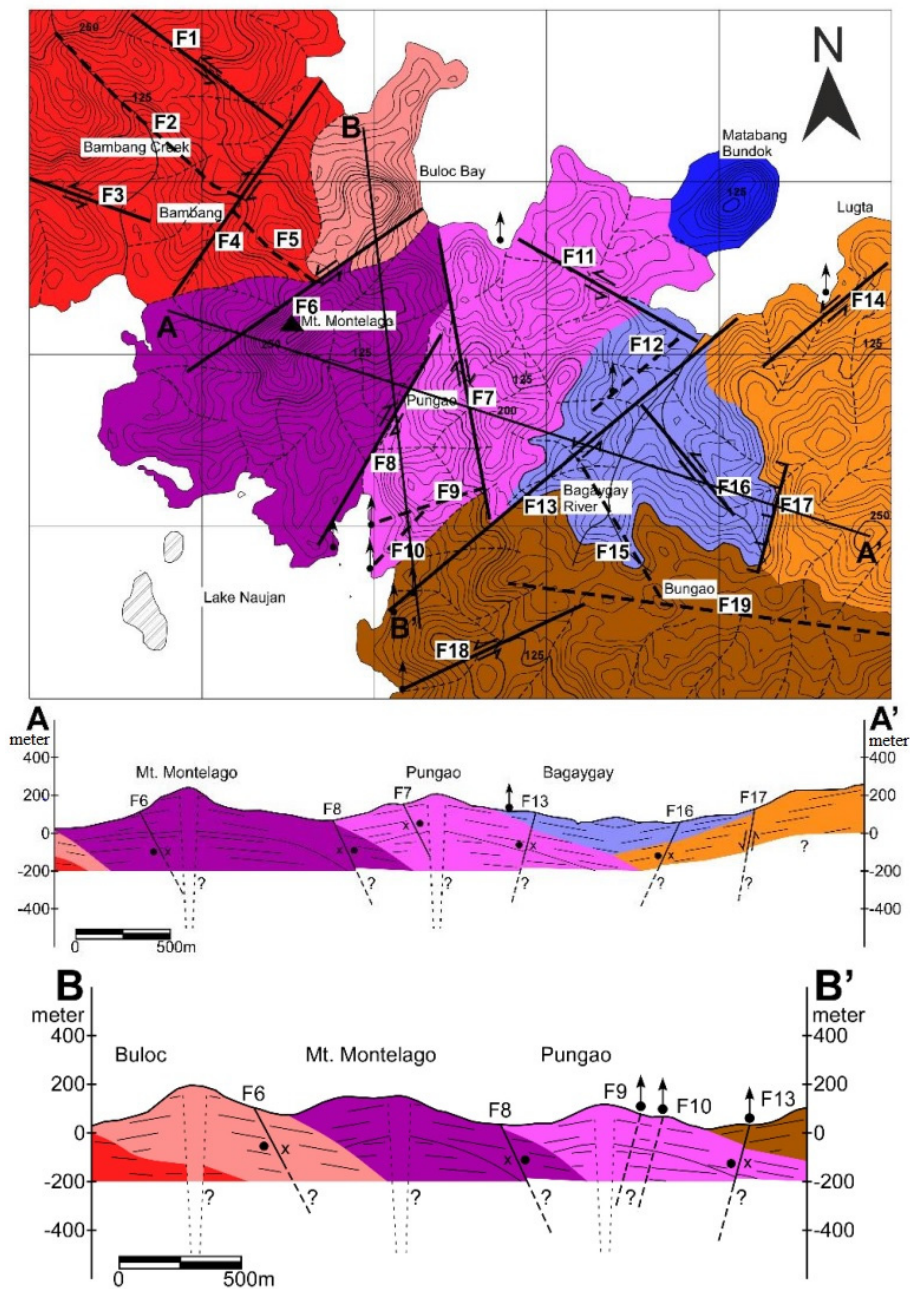


FIGURE 3: Fault system in the Montelago geothermal prospect (Asmin, et al., 2016)

At the beginning of the exploration, in 1978-1979, eight shallow temperature gradient holes with depths ranging from 195 to 305 m were drilled. Two of them (NGH-4 and NGH-6) are near the prospect. NGH-4 and NGH-6 have thermal gradients of $23^{\circ}\text{C} / 100 \text{ m}$ and $10^{\circ}\text{C} / 100 \text{ m}$, respectively. The temperature obtained in NGH-4 and the chemical composition of the Pungao springs encouraged further exploration of the prospect (SKM, 2011). From 2014 to 2016, four new wells were drilled, that is two slim holes and two deep wells. Table 2 shows the information about these wells:

The wells drilled in the prospect provided insights into the resource conditions. Among these wells, slim hole SH-02 was the only well that was able to produce. This slim hole showed an elevated concentration of NCG (non-condensable gas) but it remains unclear whether the NCG enter the wellbore at shallower depth (which could be cased-off when drilling a deeper well) or if a gas rich zone is present at greater depth. Further, the well also encountered significant calcite scaling. The formation of

TABLE 2: Montelago wells (GeothermEx, 2017)

Well name	Drilling		Total depth, (m)	Temp, (°C)	Productivity index (l/s/bar)	Injectivity index, (l/s/bar)	Remarks
	From	To					
SH-01	Dec. 11, 2014	Mar. 28, 2018	1250	180	-	0.01	No significant permeability. High level of NCG encountered and calcite scaling observed during production.
SH-02	Dec. 20, 2014	Mar. 08, 2015	1200	208	0.13	0.2	
MN-01	Oct. 26, 2015	Dec. 20, 2015	2001	136	-	4.3	No flow, but no NCG rich steam zone encountered.
MN-02	Jan. 04, 2016	Feb. 25, 2016	2150	136	-	4	No flow, but no NCG rich steam zone encountered.

amorphous silica scale is unlikely at temperatures above approximately 110°C, at lower temperatures silica oversaturation occurs. However, it is believed that the fluid produced during the test is not representative of the deeper reservoir fluid (GeothermEx, 2017). On the other hand, wells MN-01 and MN-02 appears to be the out of the reservoir zone while SH-01 confirmed the intermediate temperature of the reservoir but has too low permeability to produce.

Based on the additional information obtained from the wells, GeothermEx's (2017) report provided a conservative estimate of reservoir area of about 0.8 km² to 2.4 km². This estimate considers areas that might be acidic or too low in permeability and nonetheless implies that the reservoir is economically exploitable. Results from wells MN-01 and MN-02 show marginally economic temperatures for self-flowing wells that are too hot to pump. Additionally, based on the depths with considerable permeability and to avoid the excess risk of a long open-hole section, the report estimates the average reservoir thickness to be between 1300 m and 1700 m. The report also estimated a range of temperatures which lies between 175°C and 205°C. Other than these, the report also described the following parameters to estimate the recoverable energy of the resource as seen in Table 3:

TABLE 3: Additional parameters of GeothermEx resource assessment

Input variables	Units	Minimum	Most likely	Maximum
Porosity	(%)	3%		10%
Recovery factor	(%)	5.0%		20.0%
Volumetric specific heat of rock	(kJ/m ³)		2613	
Rejection temperature	(°C)		26	
Utilization factor	(%)		45	
Capacity factor	(%)		90	
Plant life	(years)		20	

With the information above, GeothermEx estimated that the capacity of the resource is around 15 MW and could potentially be up to 24 MW.

For this paper, the author has adopted most of the estimates made by GeothermEx (2017) while some information was changed to accommodate the design of a binary geothermal power plant that has a plant life of 30 years. Additionally, to simplify the calculation, the most likely reservoir temperature was adopted from Axelsson and Halldórsdóttir (2015) which is 190°C. It was also assumed that the thermodynamic properties of the geothermal fluid were pure water properties. To estimate the reinjection temperature the author applies the silica "rule of thumb" which entail that it is only possible to cool the water by around 100°C without risking scaling (Thórhallsson, 2005). Thus, the author uses

90°C as the reinjection temperature in this study. This report also assumes that the conversion efficiency of the system is based on the typical thermal efficiency of binary plants which is 8 to 12% (DiPippo, 2016). The parameters are summarized in Table 4.

TABLE 4: Resource assessment estimates for modelling

Input variables	Units	Minimum	Most likely	Maximum
Surface area ¹	(km ²)	0.8		2.4
Thickness ¹	(m)	1300		1700
Rock density	(kg/m ³)		2700	
Porosity ¹	(%)	3%		10%
Rock specific heat	(kJ/kg-°C)		0.9	
Temperature	(°C)	175 ¹	190 ²	205 ¹
Fluid density	(kg/m ³)	853	876	892
Fluid specific heat	(kJ/kg-°C)	4.387	4.447	4.520
Recovery factor ¹	(%)	5.0%		20.0%
Conversion efficiency ³	(%)	8.0%		12.0%
Plant life	(years)		30	
Rejection temperature ⁴	(°C)		90	

¹(GeothermEx, 2017); ²(Axelsson and Halldórsdóttir, 2015); ³(DiPippo, 2016); ⁴(Thórhallsson, 2005)

Using the information above in the Monte Carlo simulation to estimate the potential capacity of the resource the following result were obtained (Figure 4).

The prospect has the capability to provide a power output ranging from 3.4 to 12.6 MWe with the most likely power output being 8.8 MWe. There is a significant difference between the estimates made by GeothermEx (15-24 MWe) and the author. The major difference among the two lies in the rejection temperature, as the author would like to make a conservative estimate on the potential capacity of the prospect. The information gathered in Monte Carlo simulation will be used in the power plant modelling to identify the most sustainable operating capacity of the system.

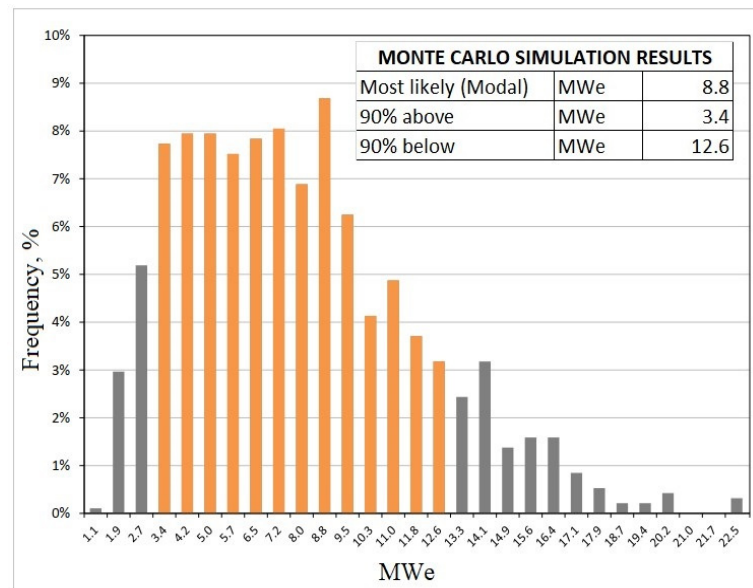


FIGURE 4: Monte Carlo simulation of the Montelago geothermal prospect

3. POWER PLANT MODELLING

This section aims to discuss the cycle of the system and to determine the optimal capacity of a generating unit that could be built with the described system. Additionally, in this section we will determine the cost of developing the prospect. The characters, symbols and abbreviations used in this model are defined in the nomenclature at the end of this report.

3.2 Thermodynamic processes

For the power plant modelling, the author designed the system by following the thermodynamic cycle shown in Figure 6 in which a straight line represents the geothermal fluid while the working fluid is represented by a dashed line. In this thermodynamic process assumptions must be made and the processes that occur at each step are listed below:

Step 1 - 4: The pressure of the working fluid remains constant while heat is added the recuperator, preheater and evaporator.

Step 4 - 5: The working fluid is expanded with an isentropic inefficiency of 82% as it exits the turbine.

Step 5 - 7: The pressure of the working fluid remains constant as it rejects heat in the recuperator and condenser.

Step 7 - 1: The working fluid is compressed with an isentropic inefficiency of 75% as it is re-pressurized and used again to repeat the cycle.

Step s-1 - s-3: The geothermal fluid is assumed to be isobaric while giving off heat in the evaporator and the preheater.

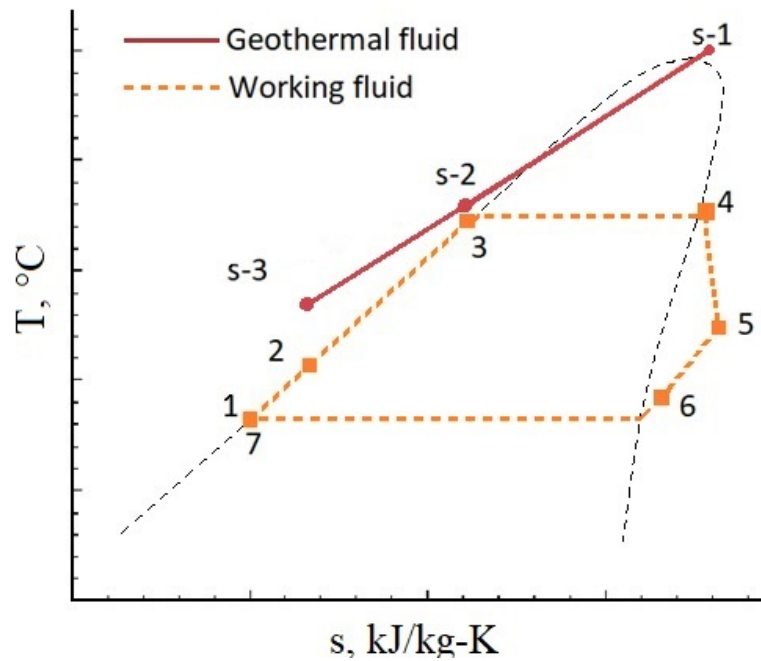


FIGURE 6: Thermodynamic process

3.3 Major components

In the schematic diagram of the model (Figure 4) several major components were identified. This section will discuss and describe the other calculations made.

3.3.1 Production well

As mentioned in Section 2.3 of this report, in the Montelago prospect there are eight shallow gradients, two slim holes and two deep wells. However, none of these well is a good candidate for power production regarding the design objectives in this report. Thus, with the parameters from the resource assessment, Table 5 summarizes the main parameters of the four producing wells that will be used in this report.

TABLE 5: Production wells description

Description	Units	Values
Well depth	(m)	2500
Well diameter casing	(in)	9 5/8
Reservoir temperature	(°C)	190
Reservoir pressure	(MPa)	1.255
Reservoir enthalpy	(kJ/kg)	807.6

According to DiPippo (2016), an intermediate-temperature geothermal resource with temperatures between 150 and 200°C can be used for electricity generation, but some wells must be pumped to provide the water required by the system. Thus, in this scenario, the production wells in this report requires pumping. However, since the described wells lacks data to calculate the power requirements for pumping, it was assumed that the water level of the well is located 200 m

below the well head and the required discharge pressure is 3.5 bar.

With those assumptions made, a line-shaft pump with a motor size of 200 kW must be used to give a flow rate of 40 kg/s. Additionally, it was assumed that the pump at 300 m depth will be kept the well running during the desired plant life (Lýdur Skúlason, project manager at Deilir Technical Service, pers. comm., 2019).

3.3.2 Heat exchanger

Heat exchangers are devices used to transfer heat from a hot fluid to a colder fluid. In the system shown in Figure 5, there are four heat exchangers (evaporator, preheater, recuperator and condenser). In the preheater and evaporator, the heat from the geothermal fluid is used to heat-up and vaporize the working fluid. In the recuperator, the heat from the exhaust from the turbine is used to heat-up the working fluid before the preheater inlet. In the condenser, the heat from the working fluid is removed and condensed by cold air. The heat transfer in the heat exchangers can be calculated based on the energy balance of hot and cold fluid as listed in Table 6.

TABLE 6: Heat transfer in the heat exchanger

Heat in components	Hot fluid	Cold fluid
$\dot{Q}_{\text{Evaporator}}$	$\dot{m}_s C_{p\text{-water}} (T_{s2} - T_{s1})$	$\dot{m}_{wf} (h_4 - h_3)$
$\dot{Q}_{\text{Preheater}}$	$\dot{m}_s C_{p\text{-water}} (T_{s3} - T_{s2})$	$\dot{m}_{wf} (h_3 - h_2)$
$\dot{Q}_{\text{Recuperator}}$	$\dot{m}_{wf} (h_6 - h_5)$	$\dot{m}_{wf} (h_2 - h_1)$
$\dot{Q}_{\text{Condenser}}$	$\dot{m}_{wf} (h_6 - h_7)$	$\dot{m}_{ct} C_{p\text{-air}} (T_{ct2} - T_{ct1})$

* C_p – heat capacity value determined using the built-in thermophysical property functions in EES

3.3.3 Turbine and generator

The turbine uses the enthalpy from the pressurized working fluid vapour and converts it into mechanical energy that will be converted into electrical energy in the generator. The power generated in the turbine is calculated with this formula:

$$\dot{W}_{Turbine} = \dot{m}_{wf} (h_4 - h_5) \quad (1)$$

When the working fluid enters the turbine, it undergoes an isentropic expansion process. However, this process does not occur without any losses, so the values are corrected using the turbine efficiency to determine the true value at the turbine outlet. The following equation is used:

$$\eta_{Turbine} = \frac{(h_4 - h_5)}{(h_4 - h_{s,5})} \quad (2)$$

The mechanical power generated by the turbine is then converted into electricity by the generator. The following equation is used to determine the generated power:

$$\dot{W}_{generator} = \dot{W}_{Turbine} * \eta_{Generator} \quad (3)$$

3.3.4 Pump

The pumps in the system are the main drivers to create flow. In this report, the modelled system has two pumps, a feed pump and a wellhead pump. The power of these pumps is calculated as follows:

$$\dot{W}_{Pump} = \frac{v_{pump,in} * \Delta P * 100}{\eta_{pump}} \quad (4)$$

3.3.5 Condenser

There are various types of condensers that can be used in ORC power plants. Choosing the suitable type of condenser is dependent on the weather and the availability of water.

The power requirements of these units were calculated using the following formula:

$$W_{fan} = \frac{v_{pump,in} * \Delta P_{air} * 100}{\eta_{pump} * \eta_{motor}} \quad (5)$$

3.3.6 Working fluid

When choosing a working fluid, several factors need to be considered. According to DiPippo (2016), the performance of a fluid is dependent on the geothermal conditions, the type of binary cycle, and any other operating or design constraint. Other factors are flammability, toxicity, chemical aggressiveness, potential hazards to the environment, and cost. Based on the factors mentioned, this report considered using either isopentane or N-pentane as a working fluid as the critical temperatures of these fluids fit the resource temperature.

Based on the so-called nose diagram (Figure 7), isopentane is the better option as it would provide more power output compared to N-pentane. The nose diagram also showed that the best pressure on the high-pressure side of the system is 13 bar as this pressure has the highest value of net power above the reinjection temperature limit.

3.4 Cost estimation

Getting an accurate estimate of the total cost of a project is difficult as each project is unique and the project's confidentiality about cost information must be considered. To get a better cost estimate, the author explored several methods including the use of empirical formulas from reference materials, estimated values from the Philippines' Department of Energy, and consultation of experienced professional with a wide background in such project. These estimation methods are described in the following sections:

3.4.1 Pre-development cost

For this report, the author adopts the seven years' cost estimation made by the DOE (2019c) for the pre-development stage or exploration stage of a geothermal project in the Philippines as illustrated in Figure 8. This cost range, represented by the shaded area on Figure 8, was based on the records and data obtained from the internal report from the DOE and varies depending on the size of the prospect area and location.

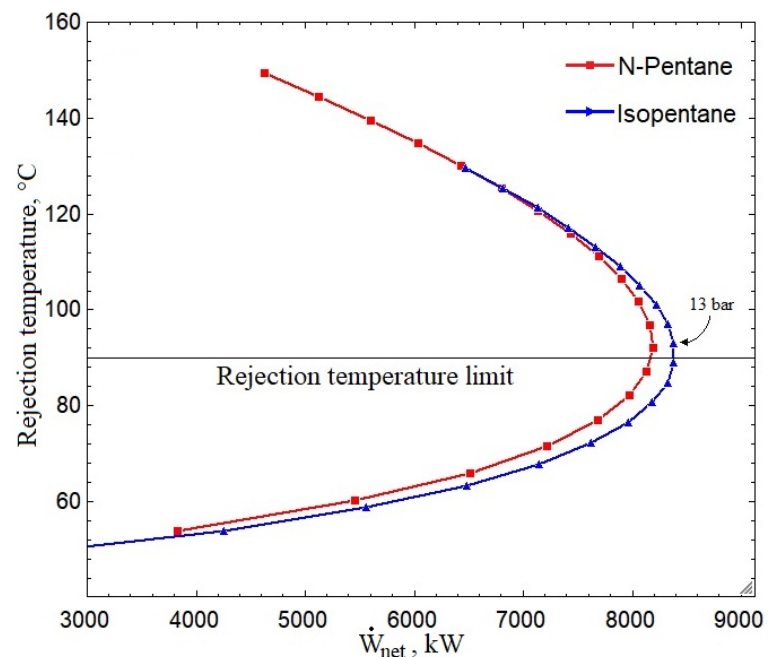


FIGURE 7: Nose diagram generated from EES (net power vs reinjection temperature)

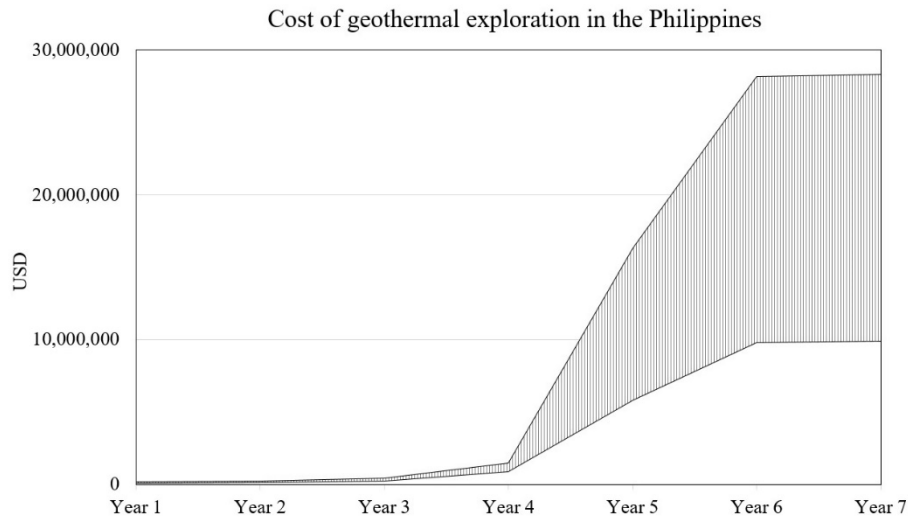


FIGURE 8: Geothermal exploration cost in the Philippines for the first seven years

Based on the report, the pre-development cost in the Philippines for seven years varies in the range USD 9 877 294 - 28 330 658 (PHP 516 780 000 - 1 482 260 000). The costs included in the report are as follows:

- Year 1 - Preparatory activities and acquisition of permits and clearances;
- Year 2 - Preliminary geoscientific studies;
- Year 3 - Detailed geoscientific surveys;
- Year 4 - Drilling preparations;
- Year 5 - Confirmatory drilling;
- Year 6 - Delineation/development drilling; and
- Year 7 - Project review and planning.

For this report, the author uses the minimum value listed in the DOE's internal report as the modelled prospect is a small binary geothermal power plant. Additionally, the computed cost estimate of a conventional well is used rather than the one provided in the report as the computed value better reflects on the cost of the project itself. Based on this, the total cost of investment for the pre-development stage, without the cost of drilling of conventional well, is USD 2 232 000 (PHP 116 780 000).

3.4.2 Drilling

The author uses the total number of wells needed using the estimation made by the International Finance Corporation (IFC). According to IFC (2013), the average well drilling success rate differs according to the phase of the project: during the exploration phase an average of 59% of wells are successful; during the development phase the average is 74%; and during the operation phase it increases to 83%. For this study, the author determines the total number of wells based on a conservative well drilling success rate of about 60%. It is also assumed that the unsuccessful or none producing wells could be used for reinjection. In a real scenario this is not always possible as some wells may not be useful for either production or reinjection. For the cost of drilling of each well, the author uses the cost estimation provided in Hance (2005):

$$C_{Drilling} = 240,785 + 210(D) + 0.019069(D)^2 \quad (6)$$

3.4.3 Major components

To get a better cost estimate of the major components of the power plant, the author explored several methods that include using empirical formulas for cost estimation from the literature and consulting

experienced professional with a wide background in such project. The cost estimation is summarized in Tables 7 and 8:

TABLE 7: Cost estimation based on literature

Component, k	Formula
Turbine	$\log_{10}(C_k) = k_1 + k_2 \log_{10}(\dot{W}_k) + k_3 [\log_{10}(\dot{W}_k)]^2$ ¹ $k_1 = 2.6259; k_2 = 1.4398; k_3 = -0.1776$ ² $k_1 = 2.2476; k_2 = 1.4965; k_3 = -0.1538$ ³ $k_1 = 2.7050; k_2 = 1.4400; k_3 = -0.1770$
Heat exchangers	$\log_{10}(C_k) = k_1 + k_2 \log_{10}(A) + k_3 [\log_{10}(A)]^2$ ¹ $k_1 = 4.6656; k_2 = -0.1557; k_3 = 0.1547$ ² $k_1 = 4.6656; k_2 = -0.1557; k_3 = 0.1547$ ³ $k_1 = 4.3247; k_2 = -0.3030; k_3 = 0.1634$
Pumps	$\log_{10}(C_k) = k_1 + k_2 \log_{10}(\dot{W}_k) + k_3 [\log_{10}(\dot{W}_k)]^2$ ¹ $k_1 = 3.3892; k_2 = 0.0536; k_3 = 0.1547$ ² $k_1 = 3.3892; k_2 = 0.0536; k_3 = 0.1547$ ³ $k_1 = 3.8700; k_2 = 0.3160; k_3 = 0.1220$
Condenser	¹ Formula from heat exchanger was used ² $C_k = 12300 * \left(\frac{\dot{Q}_k}{50}\right)^{0.76}$ ³ Formula from heat exchanger was used
Generator	¹ No formula available ² $C_k = 1,850,000 \left(\frac{\dot{W}_k}{11,800}\right)^{0.94}$ ³ No formula available

¹ El-Eman & Dincer (2013); ² Lemmens (2016); ³ Jing, et al. (2017)

TABLE 8: Estimation by an experienced professional
(Dr. Páll Valdimarsson, adjunct professor at Reykjavík University, pers. comm., 2019)

Component, k	Formula
Turbine and generator	$C_k = \dot{W}_k * 400$
Heat exchangers	$C_k = A_k * 300$
Pumps	$C_k = \dot{W}_k * 400$
Air-cooled condenser	$C_k = A_k * 600$

For the cost estimation of turbine, generator and pump, the calculations could be easily done based on the results of the power plant modelling. The area of the heat exchangers is calculated using the following formula:

$$\dot{Q} = U * A * LMTD \quad (7)$$

LMTD can be calculated following this formula:

$$LMTD = \frac{(T_{hot,in} - T_{cold,out}) - (T_{hot,out} - T_{cold,in})}{\ln \frac{(T_{hot,in} - T_{cold,out})}{(T_{hot,out} - T_{cold,in})}} \quad (8)$$

The subscripts “hot” and “cold” refer to the fluids listed in Table 9 and the subscripts “in” and “out” refers to the inlet and outlet of the heat exchanger.

The heat transfer coefficient varies widely as this value is highly dependent on the materials and the fluids in the heat exchanger. To simplify this part of the report, the following values were assumed (Dr.

Páll Valdimarsson, adjunct professor at Reykjavík University, pers. comm., 2019) (Table 9):

TABLE 9: Heat transfer coefficients

Process	Heat transfer coefficient $\frac{kW}{m^2K}$
Geothermal heat to isopentane (vapour)	0.8
Geothermal heat to isopentane (boiling)	1.2
Geothermal heat to isopentane (liquid)	0.5
Cooling air to isopentane (vapour)	0.5
Cooling air to isopentane (dew)	1.0
Isopentane (vapour) to isopentane (liquid)	0.3

The result of cost estimates from various source are presented in Appendix II. The results obtained from different literature sources vary making it harder to get a good cost estimate for the component.

In consultation with the advisors, the author uses the cost estimates presented in Table 8, as this approach is simple and updating the cost estimate according to the market price is easier compared to the formulas presented in Table 7 of which some were already outdated.

3.4.4 Operation and maintenance (O&M)

Cost of O&M is 20% to 25% of the purchased equipment cost (PEC) (El-Eman and Dincer, 2013). For this report, the author assumes that the annual cost of O&M is equal to the 20% of PEC.

3.4.5 Total cost of investment

The total cost of investment is the sum of the Fixed Capital Investment (FCI) and other outlays. The FCI is the total of direct cost and indirect cost. The direct cost (DC) is composed but not limited to the following: purchased equipment cost, purchased equipment installation, piping, instrumentations and controls, electrical equipment and materials, land, civil, structural, and architectural work, and service facilities. Indirect cost, on the other hand, is composed but not limited to the following: engineering and supervision, construction costs including contractor's profit, and contingencies. The other outlays costs are composed of the following: start-up cost, working capital, cost of licensing, research and development, and allowance for funds used during construction. The cost for the FCI used in this report is summarized in Table 10.

3.5 Profitability evaluation

In each project, it is important to evaluate the profitability of the investment before capital is invested. However, calculating the profitability of an investment is complex as there are associated risks and uncertainties. Analysing those risk and uncertainties is not covered in this report. Therefore, to determine the profitability of the model, the author adopts the deterministic investment analysis presented in Bejan et al. (1996). In this analysis, the following was assumed:

1. There is a perfect capital market: the supply of funds is unrestricted;
2. There is complete certainty about investment outcomes;
3. Investment projects are indivisible; and
4. Profitability of one project does not in any way affect the profitability of any other project.

After setting up the conditions for the profitability evaluation, the Net Present Value (NPV) method and the Internal Rate of Return (IRR) method are used for analysis.

TABLE 10: Total cost of investment

Cost breakdown	Cost ranges ¹	Value adopted from Lukawski (2009) ²
I. Fixed capital investment		
A. Direct costs		
1. Onsite costs		
-Purchased equipment cost	15 - 40% of FCI	Sum of the cost of the equipment determined ³
-Purchased equipment installation	20 - 90% of PEC 6 - 14% of FCI	6% of PEC
-Piping	10 - 70% of PEC 3 - 20% of FCI	7% of PEC
-Instrumentation and controls	6 - 40% of PEC 2 - 8% of FCI	5% of PEC
-Electrical equipment and materials	10 - 15% of PEC 2 - 10% of FCI	4% of PEC
2. Offsite costs		
-Land	0 - 10% of PEC 0 - 2% of FCI	Negligible
-Civil, structural, & architectural work	15 - 90% of PEC 5 - 23% of FCI	7% of PEC
B. Indirect cost		
1. Engineering and supervision	25 - 75% of PEC 6 - 15% DC 4 - 21% FCI	10% of PEC ⁴
2. Construction cost with contractor's profit	15 of DC 6 - 22% of FCI	3% of DC
3. Contingencies	8 - 25% of the sum of above costs 5 - 20% of FCI	3% of FCI
II. Other outlays		
A. Start-up costs	5 - 12% of FCI	1% of FCI
B. Working capital	10 - 20% of TCI	3% of PEC
C. Allowance for funds used in construction		Negligible

¹ Bejan et al. (1996); ² For further information on the estimation made refer to Lukawski (2009);

³ The PEC is based on the cost estimation made in this report;

⁴ The author uses 10% of PEC rather than 6% in Lukawski (2009), as the author believes that the assigned value is more reasonable in the Philippine setting.

3.6 Power plant model setup

The selected prospect is currently one of the most advanced projects in the pre-development stage in the Philippines. Despite of this, assumptions have to be made for the power plant model:

1. Well characteristics:
 - a. No. of required producing wells = 4;
 - b. Reservoir temperature = 190°C;
 - c. Reservoir pressure = 12.55 bar.
2. The temperature in the system plays a very important role in economics and the performance of

the power plant. For this report, the following temperatures were assigned in the model:

- a. $T_{\text{condensation}} = 47^{\circ}\text{C}$;
 - b. $T_{\text{pinch}} = 4^{\circ}\text{C}$;
 - c. $T_{\text{vap,sh}} = 2^{\circ}\text{C}$;
 - d. $T_{\text{boilingmargin}} = 2^{\circ}\text{C}$;
 - e. $T_{\text{cond,air,in}} = 27^{\circ}\text{C}$;
 - f. $T_{\text{cond,air,out}} = 37^{\circ}\text{C}$;
 - g. $T_{\text{recuperator,out}} = 52^{\circ}\text{C}$.
3. Efficiencies used in this report were assumed to be:
 - a. Turbine = 82%;
 - b. Generator = 95%;
 - c. Pump = 75%;
 - d. Condenser fan = 65%;
 - e. Fan motor = 98%.
 4. As discussed in Section 3.3.6, the working fluid used in this report is isopentane at high pressure (13 bars).
 5. Due to high air humidity in the prospect area, using an ACC would be more cost effective compared to evaporative cooling condenser.
 6. Change in air pressure in the condenser is assumed to be 0.0017 bar.
 7. As mentioned on Section 3.3, each well will be equipped with a well head pump that has a mass flow rate of 40 kg/s and can deliver up to 3.5 bar.
 8. While a high amount of NCG is present in fluids from SH-02, according to GeothermEx (2017), it is believed that the fluid produced during the test is not representative of the deeper reservoir fluid.
 9. Thus, for the modelling the author assumed that the NCG content of the reservoir is negligible.
 10. The geothermal fluid was assumed to be pure water.
 11. To avoid silica saturation, the rejection temperature of the geothermal brine should be higher than 90°C .
 12. Pressure loss due to friction in the system was disregarded.
 13. For the profitability equation, the following values were assumed:
 - a. Effective discount rate = 10%;
 - b. Annual operations period = 340 days.

3.7 Design constraints

According to Clarke (2014), a binary geothermal power plant has four (4) major constraints that must be met to ensure effective plant operations. The constraints are as follows:

1. The lower limit of the quality of vapour as it exits the turbine should be greater than 97% to prevent excessive damage of the turbine blades.
2. The upper limit of evaporator pressure is two (2) MPa or 20 bars to limit the mechanical stresses on the plant components and to ensure that the fluid remains sub-critical throughout the cycle.
3. The outlet temperature of the geothermal brine should exceed the working fluid temperature at the inlet of the preheater by at least the pinch point temperature difference.
4. The problem of scaling should be considered.

4. THERMOECONOMIC MODELLING

In this section, the author describes the background of thermoeconomic modelling which is used to determine the minimum cost of generation and to give an insight on which components could be optimized to further improve the system. The parameters used in this model are defined in the nomenclature in the back of this report.

4.1 Fundamentals of thermoeconomics

Thermoeconomics is the combination of energy analysis and economic principles and is used to get information that is not available through conventional energy analysis and economic evaluations but crucial to the design and operation of a cost-effective system (Bejan et al., 1996). It is also used to balance expenditure or capital cost and exergy cost to estimate the minimum cost of the plant product (Kotas, 1985). The cost balance expresses that the cost rate of the product, p , is equal to the sum of the rate of expenditures or capital cost and the cost rate of fuel, f :

$$\dot{C}_{p,total} = \dot{C}_{f,total} + \dot{Z}_{total}^{CI} + \dot{Z}_{total}^{OM} \quad (9)$$

4.2 Component cost rates

Each component has two cost rates, capital investment, CI and O&M. The cost rate of the capital investment of a component is the product of the present worth factor for specific components of plant equipment and the capital recovery factor (CRF) divided by the annual period of operation time τ of the plant:

$$\dot{Z}_k^{CI} = \frac{PW_k * CRF}{\tau} \quad (10)$$

The present worth factor is:

$$PW_k = C_k - \frac{S_k}{(1 + i_{eff})^n} \quad (11)$$

The CRF is:

$$CRF = \frac{(1 + i_{eff})^n}{(1 + i_{eff})^n - 1} \quad (12)$$

To obtain the O&M cost rate of a component, the component's O&M cost should be expressed first to its levelized value. This concept of levelization is defined as the use of time-value-of-money arithmetic to convert a series of varying quantities to a financially equivalent constant quantity or annuity over a specified time interval. The levelized value of O&M is expressed through the following equation:

$$C_{l,O\&M} = C_{O\&M} * CELF = C_{O\&M} * \left(\frac{k * (1 - k^n)}{1 - k} * CRF \right) \quad (13)$$

where k is calculated as:

$$k = \frac{1 + r_n}{1 + i_{eff}} \quad (14)$$

In this report, it is assumed that the nominal rate r_n is 4%. The cost rate of O&M for a specific component is:

$$\dot{Z}_k^{OM} = \frac{C_{l,O\&M} * CRF}{\tau} * \frac{C_k}{C_{PEC}} \quad (15)$$

4.3 Exergy analysis

Exergy analysis is an important tool for design and analysis of thermal systems and is used as the basis of thermoeconomics. Exergy analysis is used to improve the effectiveness of energy resource use, as it enables the determination of the location, cause, and true magnitude of waste and loss (Bejan et al.,

1996). Exergy is defined as the maximum portion of energy that can be converted into work (Valdimarsson, 2010) while the none converted part is called anergy. This means that the specific exergy rate for a stream is limited to the environmental state of the process and is expressed as:

$$e_k = (h_k - h_0) - T_0(s_k - s_0) \quad (16)$$

and the exergy rate is expressed as:

$$\dot{E}_k = m_k * e_k \quad (17)$$

In this report, the environmental state or the dead state, which is represented by subscript 0 in Equation 16, is identified as the ambient temperature.

In thermoeconomics, it is important to take note of the hidden cost. This cost is associated with exergy destruction which can be revealed through thermoeconomic analysis. The exergy destruction is expressed as:

$$\dot{E}_{f,k} = \dot{E}_{p,k} + \dot{E}_{l,k} + \dot{E}_{d,k} \quad (18)$$

The Exergy rate of component associated with fuel, $\dot{E}_{f,k}$, refers to the exergy coming from the geothermal system. The Exergy rate of component associated with product, $\dot{E}_{p,k}$, refers to the exergy produced by the component. The Exergy rate of loss of component, $\dot{E}_{l,k}$, refers to the exergy stream that flows from the outside of the component and was not used by other components in the system. The Exergy rate of destruction of component, $\dot{E}_{d,k}$, refers to the exergy destroyed in the stream.

4.4 Exergy costing

Exergy costing is an approach in thermoeconomics in which it is believed that exergy is the only rational basis for assigning costs to the interactions that a thermal system experiences with its surroundings and with the sources of inefficiencies within it (Bejan et al., 1996). It is also an effective tool to evaluate the cost effectiveness of thermals systems, used to evaluate and enhance the performance from both an economic and exergetic point of view (Adefila et al., 2015).

Exergy costing is associated with the entering and exiting of streams and their associated rates of exergy transfer. This involved cost balances of entering and exiting streams plus the appropriate charges due to capital investments and operating and maintenance expenses on each component separately. This is expressed in the following equation.

$$\sum_e \dot{C}_{e,k} + \dot{C}_{w,k} = \dot{C}_{q,k} + \sum_i \dot{C}_{i,k} + \dot{Z}_k \quad (19)$$

The cost of the stream is expressed as:

$$\dot{C}_k = c_k * \dot{E}_k \quad (20)$$

Thus, Equation 19 could be re-written as:

$$\sum_e c_{e,k} \dot{E}_{e,k} + c_{w,k} \dot{E}_{w,k} = c_{q,k} \dot{E}_{q,k} + \sum_i c_{i,k} \dot{E}_{i,k} + \dot{Z}_k \quad (21)$$

When the component receives power, $\dot{C}_{w,k}$ would be moved to the right-hand side of the equation. $\dot{C}_{q,k}$ would be transferred to the left side if there is a heat transfer from the component.

When analysing a component, it is important to remember that the cost of exergy is based on the stream that is entering and exiting a component. We can assume that the exergy cost per unit is known for all

entering streams since they are the cost of the stream exiting the previous component and/or the cost of investment of the component. The remaining unknown variable is the exergy cost that exits the component. Additionally, when calculating exergy costing, it is important to consider the cost per exergy unit. Lastly, since the exergy exiting a component contains the cost of stream exiting a previous component, it is important to define a break point to break the loop. In this report, the author selected the inlet of the pump (point 7 on Figure 5) as the break point of the system.

The first stream to analyse is in the feed pump. The first stream has one inlet stream, one outlet stream and one power stream for work done by the pump on the system. The cost balance is calculated using the following equation:

$$\dot{C}_{pump,out} = \dot{C}_{pump,in} + \dot{C}_{pump,w} + \dot{Z}_{pump} \quad (22)$$

As mentioned earlier, the pump inlet is the break point. Therefore, the cost at pump inlet equals zero. Additionally, to determine the cost rate of pump power, an auxiliary equation is used to calculate the cost per exergy unit for the net power exported from the system while power input in the pump remains constant.

$$\dot{C}_{pump,in} = 0 \quad (23)$$

$$\frac{\dot{C}_{pump,w}}{W_{pump}} = \frac{\dot{C}_{turbine,w}}{W_{turbine}} \quad (24)$$

The second stream of the working fluid is in the recuperator. In this stream, there are two (2) inlet streams and two outlet streams. The cost balance in the recuperator is as follows:

$$\begin{aligned} \dot{C}_{recuperator,hps,out} + \dot{C}_{recuperator,lps,out} \\ = \dot{C}_{pump,out} + \dot{C}_{turbine,out} + \dot{Z}_{recuperator} \end{aligned} \quad (25)$$

In this stream, there are two outlet streams, a high-pressure side (hps) and a low-pressure side (lps), therefore, an additional equation must be added. According to Bejan et al. (1996), the purpose of a heat exchanger is to heat the cold stream and exergy is removed from the hot stream. This means that the cost per exergy unit in the hot stream remains constant.

$$C_{recuperator,lps,out} = C_{turbine,out} \quad (26)$$

Before analysing the stream in the preheater and evaporator, the cost of stream of the source should be calculated since it is added to the cost in these two components. When analysing the cost rate in the production well, it should be noted that the cost rate in the reservoir is zero since the geothermal fluid from the reservoir is natural to the environment and assumed to be free of cost. With this, the following equation for the cost balance in the production well can be formulated:

$$\dot{C}_{evaporator,s,in} = \dot{Z}_{well,production} + \dot{C}_{reservoir,s} \quad (27)$$

After passing the reservoir, the stream goes to the evaporator and the geothermal fluid enters a heat exchanger. Similarly, to what was described for the second stream of the working fluid, the cost per exergy unit in this hot stream remains constant:

$$C_{evaporator,s,in} = C_{evaporator,s,out} \quad (28)$$

The next stream of the geothermal fluid is in the preheater. In the preheater, the cost rate of geothermal fluid entering the preheater is already identified and the cost rate exiting the preheater is equal to the cost rate of the reinjection well. The cost rate of the reinjection well is expressed as:

$$\dot{C}_{preheater,s,out} + \dot{C}_{reservoir,s} + \dot{Z}_{well,reinjection} = 0 \quad (29)$$

According to the cost balance of the reinjection well, all cost rates are entering the component. This means that the value obtained at the preheater outlet is negative. This suggests that the cost of the reinjection well would also be carried out in the preheater in the system.

As the cost rates in the geothermal fluid side are now defined, the cost balance in the preheater in the working fluid side can be calculated. In the preheater, there are two outlet streams and two (2) inlet streams:

$$\begin{aligned}\dot{C}_{preheater,s,out} + \dot{C}_{preheater,wf,out} \\ = \dot{C}_{evaporator,s,out} + \dot{C}_{recuperator,hps,out} + \dot{Z}_{preheater}\end{aligned}\quad (30)$$

After the preheater, the next stream is in the evaporator. This evaporator has two outlet streams and two (2) inlet streams:

$$\begin{aligned}\dot{C}_{evaporator,s,out} + \dot{C}_{evaporator,wf,out} \\ = \dot{C}_{evaporator,s,in} + \dot{C}_{preheater,wf,out} + \dot{Z}_{evaporator}\end{aligned}\quad (31)$$

After the evaporator, the next stream is in the turbine. In this stream, there is one outlet stream, one (1) inlet stream and one (1) work done on the turbine by the system. The cost balance in the turbine is expressed as:

$$\dot{C}_{turbine,out} + \dot{C}_{turbine,w} = \dot{C}_{evaporator,wf,out} + \dot{Z}_{recuperator}\quad (32)$$

In this equation, there are two (2) exiting streams, one is the turbine outlet and the work done in the turbine. In this scenario, an auxiliary relation is required. According to Bejan et al. (1996), since the purpose of a turbine is to generate power, the exergy rate spent to generate the power and the exiting exergy rate at the turbine would not change since cost would change only if exergy was added to the working fluid during the turbine expansion. Therefore:

$$C_{evaporator,wf,out} = C_{turbine,out}\quad (33)$$

After the turbine, the stream enters the low-pressure side of the recuperator which was described earlier. After the recuperator, the stream enters the last component of the system, the air-cooled condenser (ACC), before the cycle is repeated. In the condenser, there are two outlet streams, two inlet streams and one work done by the fan in the turbine. The cost balance in this component is expressed as:

$$\dot{C}_{ACC,wf,out} + \dot{C}_{ACC,air,out} = \dot{C}_{recuperator,tps,out} + \dot{C}_{ACC,air,in} + \dot{C}_{ACC,w} + \dot{Z}_{ACC}\quad (34)$$

In this cost balance, it could be concluded that the $\dot{C}_{ACC,wf,out}$ contains all the cost rate of the system, except for the cost rate of the work done in the turbine and other cost rates outside the major components. With this, the minimum cost of product or electricity can be expressed as:

$$\dot{C}_{electricity} = \dot{C}_{ACC,wf,out} + \dot{C}_{turbine,w}\quad (35)$$

and in USD/kWh, that is:

$$\text{Minimum cost of generation(USD/kWh)} = \frac{\dot{C}_{electricity} * 3600}{\dot{W}_{net}}\quad (36)$$

4.5 Cost of exergy destruction

As mentioned in section 4.3, there are costs that are associated with the cost of exergy loss and exergy destruction. The cost of exergy loss can be expressed as:

$$\dot{C}_{p,k} = \dot{C}_{f,k} - \dot{C}_{l,k} + \dot{Z}_k\quad (37)$$

And in terms of unit cost:

$$c_{p,k}\dot{E}_{p,k} = c_{f,k}\dot{E}_{f,k} - \dot{C}_{l,k} + \dot{Z}_k \quad (38)$$

This cost of exergy loss is associated to the monetary loss that is ejected from the system to the surroundings. Using Equation 23 together with Equation 18, the cost of exergy destruction can be described as follows:

$$c_{p,k}\dot{E}_{p,k} = c_{f,k}\dot{E}_{p,k} + (c_{f,k}\dot{E}_{l,k} - \dot{C}_{l,k}) + \dot{Z}_k + c_{f,k}\dot{E}_{d,k} \quad (39a)$$

$$c_{p,k}\dot{E}_{f,k} = c_{f,k}\dot{E}_{f,k} + (c_{p,k}\dot{E}_{l,k} - \dot{C}_{l,k}) + \dot{Z}_k + c_{p,k}\dot{E}_{d,k} \quad (39b)$$

In Equation 39a, it is assumed that the product $\dot{E}_{p,k}$ is fixed and that the unit cost of fuel $c_{f,k}$ is independent to the exergy destruction. This implies that the cost of exergy destruction is equal to the product of cost of fuel and exergy destruction:

$$\dot{C}_{d,k} = c_{f,k}\dot{E}_{d,k} \quad (40a)$$

In Equation 39b, on the other hand, it is assumed that the fuel $\dot{E}_{f,k}$ is fixed and that the unit cost of the product $c_{p,k}$ is independent of the exergy destruction and expressed as:

$$\dot{C}_{d,k} = c_{p,k}\dot{E}_{d,k} \quad (40b)$$

For this report, the author uses Equation 40b since the fuel rate from the geothermal system is assumed to be fixed.

The exergy destruction and exergy loss provide thermodynamic measures of system inefficiencies. These inefficiencies can be compared to the total exergy rate of the fuel of the system which is given as:

$$y_d = \frac{\dot{E}_{d,k}}{\dot{E}_{f,total}} \quad (41)$$

$$y_l = \frac{\dot{E}_{l,k}}{\dot{E}_{f,total}} \quad (42)$$

4.6 Relative cost difference

The relative cost difference r_k expresses the relative increase of cost per exergy unit between the fuel and product. This variable is used for iterative cost optimization where the objective is to minimize the relative cost difference instead of minimizing the cost per exergy unit of the component to reveal the real cost sources. This variable is can be expressed as:

$$r_k = \frac{1 - \epsilon_k}{\epsilon_k} + \frac{(\dot{Z}_{CI,k} + \dot{Z}_{OM,k})}{c_{f,k}\dot{E}_{p,k}} \quad (43)$$

Exergetic efficiency ϵ_k is:

$$\epsilon_k = \frac{\dot{E}_{p,k}}{\dot{E}_{f,k}} = 1 - \frac{\dot{E}_{d,k} + \dot{E}_{l,k}}{\dot{E}_{f,k}} \quad (44)$$

The exergetic efficiency is used to determine how well the exergy was utilized in the system. Exergetic efficiencies of a binary power plants is usually within the range from 17.2 to 53.9% which is roughly three to five times higher than the thermal efficiency which ranges from 2.1 to 10.3% (Haraldsson, 2016).

4.7 Exergoeconomic factor

The ratio of the non-exergy-related cost to the total cost is the exergo-economic factor (f_k):

$$f_k = \frac{\dot{Z}_k}{\dot{Z}_k + c_{f,k}(\dot{E}_{d,k} + \dot{E}_{l,k})} \quad (45)$$

A low exergo-economic factor implies that cost saving in the entire system could be achieved by improving the components' efficiency through the reduction of exergy destruction even if the capital investment for this component increases. On the other hand, a high value of this factor suggests that the capital investment could be lessened even if this would decrease the exergetic efficiency. For heat exchangers the factor is typically lower than 55%, for compressor and turbines it lies between 35 to 75%, and for pumps it is typically above 70% (Bejan et al., 1996).

4.8 Thermoeconomic model setup

To develop the thermoeconomic model, the author assumed the following:

1. It was assumed that the operation of the power plant is at steady state.
2. The environmental state of the system is 27 C° and 1 bar_a.
3. To simplify the exergy cost, all the streams that come from or discharge into the natural environment are set to zero cost.
4. Since the cost estimates used in this report were based to some extent on the price on the market, the author will neglect the salvage value in the calculations to provide a more conservative estimate.
5. To determine the cost rate of components that consume electricity (feed pump and air-cooled condenser), an auxiliary equation is added as the cost per exergy unit for the net power exported from the system and power input remains constant.
6. Parasitic load of the major components are the only auxiliary loads considered in this model. Other components and other loads outside the power plant, such as the well head pump, were not considered.

5. RESULTS AND DISCUSSIONS

5.1 Power plant modelling

In geothermal power plant modelling the power plant design is mainly limited, among other factors, by the geothermal resource and climate in the area. The parameters described in Section 3.10 and the constraints set in Section 3.11 served as the foundation of the model. With these considerations, the author developed a model using the Engineering Equation Solver (EES) software. The result of the modelling shows the optimal power output of the system and is illustrated the power plant block diagram in Figure 9.

The wells were considered to deliver 160 kg/s of 190°C hot water to the power plant. The heat from the geothermal fluid is transferred to the pressurized isopentane through the evaporator and preheater before it is reinjected. After the heat transfer, the isopentane boils and becomes slightly superheated reaching temperatures of up to 131.5°C. This superheated isopentane is used to drive the turbine to generate 9390 kW. After passing the turbine, the fluid remains superheated, but its pressure drops to 1.877 bar. This superheated vapour will then go to the recuperator to transfer heat to the working fluid that is located between the feed pump and the preheater. The recuperator also helps to decrease the temperature in the system prior to the ACC. Using ambient air, the ACC will now condense the isopentane at 47°C. Then, this condensed fluid is pumped back at 13 bar and the cycle is repeated. The cost of exergy \dot{C} will be discussed in the thermoeconomic model.

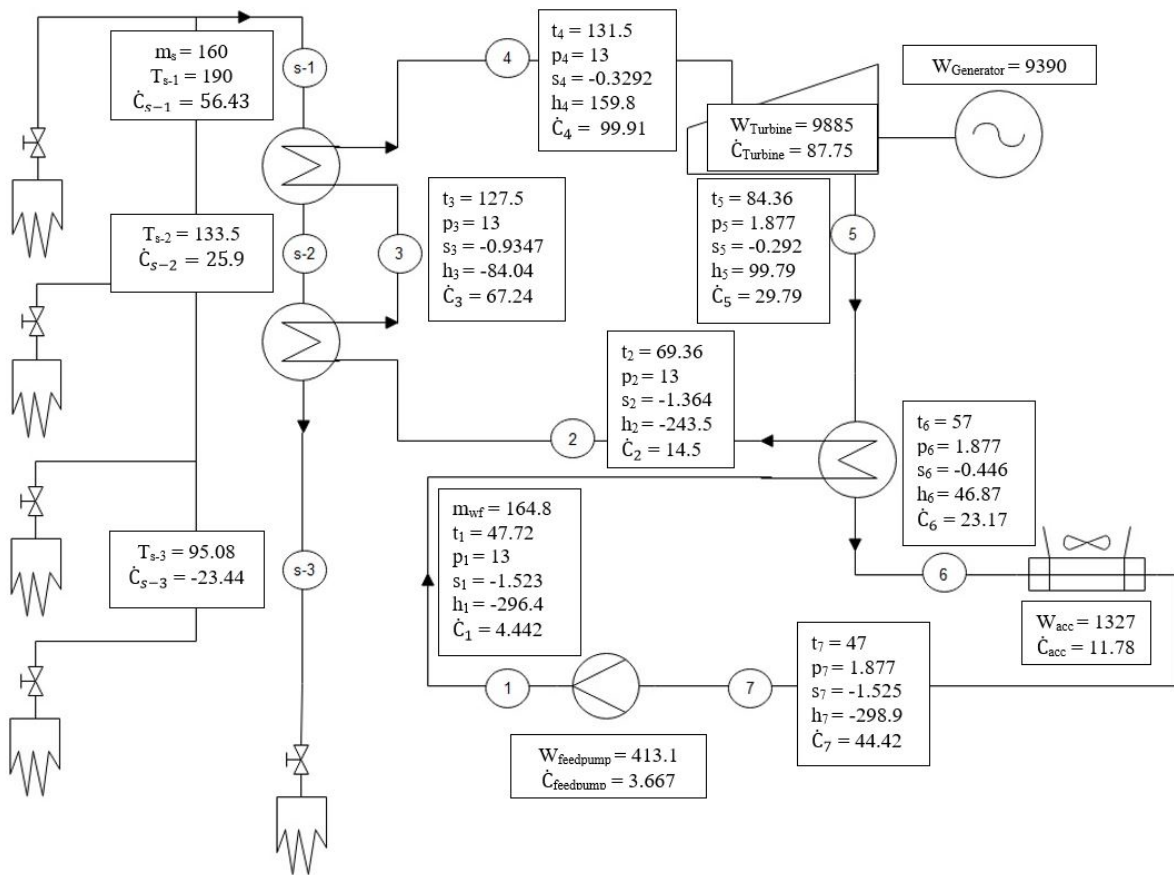


FIGURE 9: Power plant block diagram

The modelled power plant has a parasitic load of 1327 kW in the ACC and of 413.1 kW in the feed pump which reduces the power output to 7650 kW. With this, the thermal efficiency of the system is calculated to be 5.92%. To further understand the thermal efficiency a Sankey diagram is used to illustrate the heat flow in the system (Figure 10).

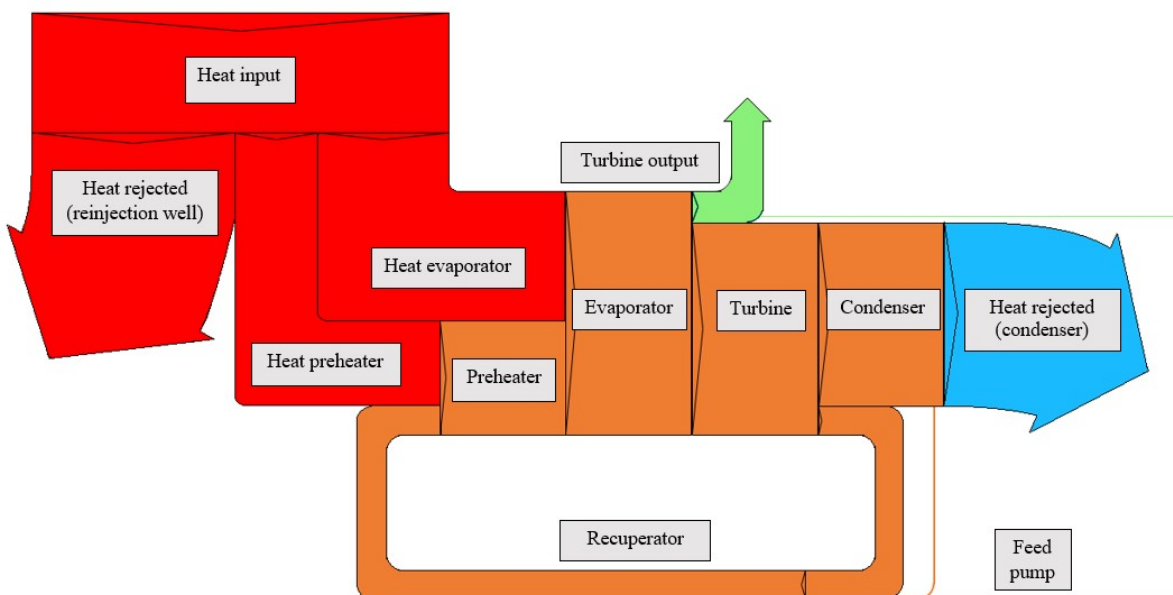


FIGURE 10: Sankey diagram of the system

The Sankey diagram is a representation of the heat flow in the system where the length of the triangle on the side of the box represents the amount of heat flow in each component. This allows a visualization of the areas that mainly affects the thermal efficiency of the power plant. One of the significant observations that can be made in the diagrams is that most of the unused heat is the reinjected heat in the reinjection well and the ACC. However, optimizing the system to use this waste heat to generate more electricity would not be easy because of the constraints on the geothermal fluid and the environment that were mentioned. In the diagram, it can also be seen that the recuperator plays a significant role through recovering waste heat and feeding it back into the system. Based on this model, the cost of developing the prospect was also calculated. The calculated cost is summarized in Table 11.

TABLE 11: Cost of developing the prospect

Description	Cost (in USD)
A. Pre-development cost	2 232 000
B. Drilling cost	19 470 000
1 Well head pump	320 000
C. Fixed Capital Investments	
1 <i>Direct cost</i>	
<i>Onsite</i>	
PEC -Purchased Equipment Cost	7 815 000
- Condenser	1 979 000
- Evaporator	455 000
- Feed Pump	165 000
- Preheater	727 000
- Recuperator	732 000
- Turbine-generator	3 756 000
Installation of PEC	469 000
Piping	547 000
Instrumentation and controls	391 000
Electrical equipment and materials	313 000
<i>Offsite costs</i>	
Land	Negligible
Civil, structural, and architectural work	547 000
2 <i>Indirect cost</i>	
Engineering and supervision	782 000
Construction cost including contractor's profit	302 000
Contingencies	345 000
D. Other outlays	
Start-up costs	96 000
Working capital	234 000
Allowance for funds used during construction	Negligible
E. Total Cost of Investment	33 562 000
F. Annual O&M cost	1 563 000

The total cost of investment and the annual O&M cost of the prospect is 33.6 and 1.56 Million USD (MUSD), respectively. The major cost of development is the drilling of wells followed by the total PEC. Therefore, the cost of development of the prospect adds up to 3574 USD/kW. This cost analysis will be further discussed in the thermoeconomic modelling.

After determining the generated net power and the cost of development, the NPV and IRR of the system were calculated (Figure 11). Based on the profitability evaluation, the project will have a positive NPV when the tariff is higher than 8.26 USDcents/kWh and a calculated IRR of 10% which is the break-even point of the system.

5.2 Thermoconomics modelling

To create a thermo-economic model, the author uses the information gathered in the power plant model and the parameters discussed in section 4.8. Like the power plant modelling, the author uses the EES to generate the thermo-economic model. The result of the modelling for the cost of components and exergy analysis is presented in Table 12.

Based on the information presented, the production and reinjection wells require the largest total investment and O&M cost in the system followed by the turbine. The analysis of the cost rates will be further discussed in the

latter part of this section. In the exergy analysis, the exergy rates were separated into four (4) columns: in, out, stream of power, and destruction. Additionally, the exergy rates in the heat exchangers were separated. Presenting the exergy rates in this manner makes it easier to interpret the exergy flow in the system. To further understand the exergy flow in the system, the exergy rates in Table 10 were illustrated using a Grassman diagram (Figure 12).

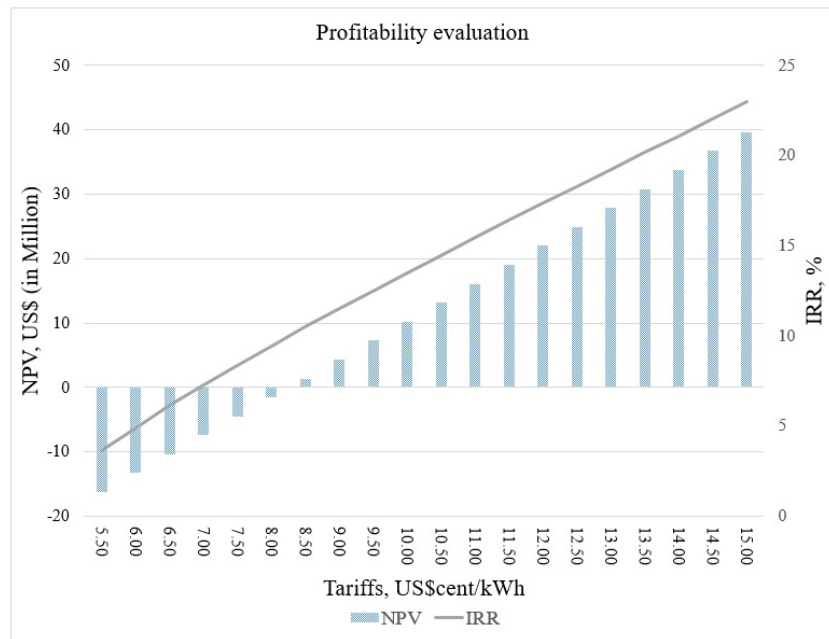


FIGURE 11: Profitability evaluation

TABLE 12: Thermo-economic model

Component k	Z _{ci} (10 ³ , USD/s)	Z _{O&M} (10 ³ , USD/s)	Z _k (10 ³ , USD/s)	E _{in} (kW)	E _{out} (kW)	E _w (kW)	E _d (kW)
Production well	56.086	0.346 ¹	56.432	0.00	22 699.00	-	-
Reinjection well	23.44	0	23.44	4 522.00	0.00	-	-
Feed pump	0.5967	0.1786	0.7753	270.30	586.30	413.10	96.99
Recuperator	2.644	0.7916	3.4356				
High-pressure side				586.30	1 415.00	-	277.60
Low-pressure side				4 980.00	3 874.00	-	-
Preheater	2.626	0.7862	3.4122				
GF side ²				10 416.00	4 522.00	-	-
WF side ³				1 415.00	6 473.00	-	835.30
Evaporator	1.643	0.492	2.135				
GF side ²				22 699.00	10 416.00	-	-
WF side ³				6 473.00	16 704.00	-	2 053.00
Turbine	13.56	4.061	17.621	16 704.00	4 980.00	-9 885.00 ⁴	1 839.00
Condenser	7.148	2.14	9.288				
WF side ³				3 874.00	270.30	-	519.00
Air side				0.00	4 412.00	1 327.00	-

¹ Cost of O&M at the well head pump; ² Geothermal fluid side; ³ Working fluid side

⁴ The negative value indicates the value of exergy going out of the component.

*The parameters are defined in the nomenclature at the back of this report.

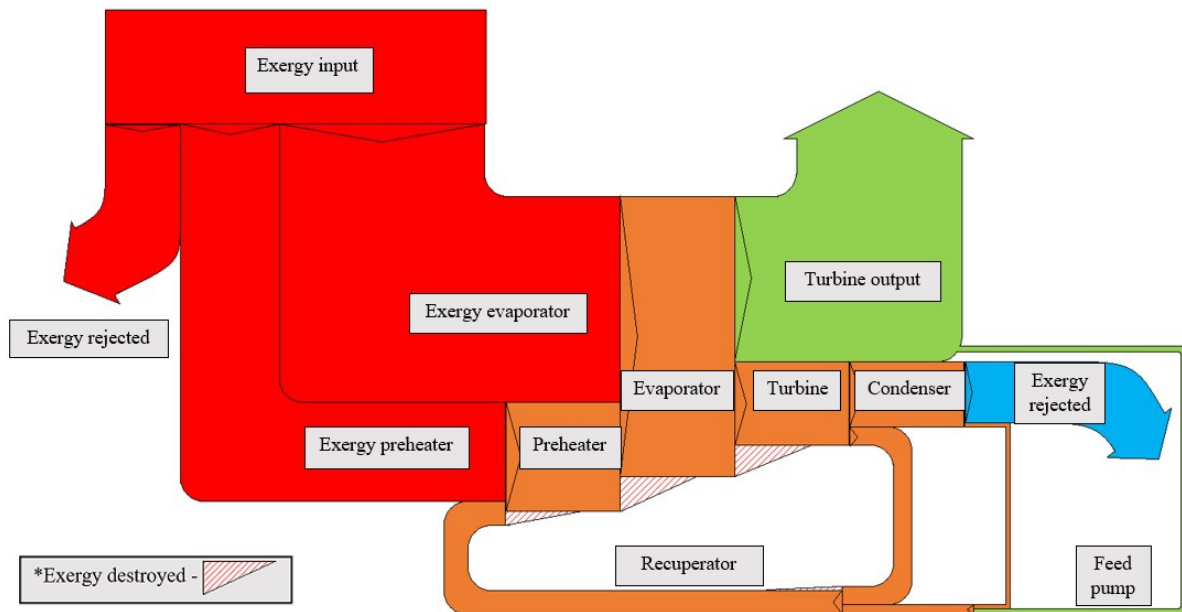


FIGURE 12: Grassman diagram of the system

The Grassman diagram shows the exergy flow in the system. The length of the triangle on the side of a box represents the amount of exergy flow in each component. The diagram shows that the effectiveness of the system in converting the exergy is high and reflects the exergetic efficiency of the power plant which is 43.55%. It could also be observed that there was significant exergy destruction in the evaporator and the turbine.

The analysis made with the Grassman diagram is important because, as mentioned in previous sections, it is used to balance between expenditure or capital cost and exergy cost to estimate the minimum cost of the plant product. With this definition, the author used the exergy cost, presented in Figure 9, to determine the minimum cost of generation. To illustrate the relationship between the exergy cost and the minimum cost of generation, the author uses the Value Flow diagram in Figure 13.

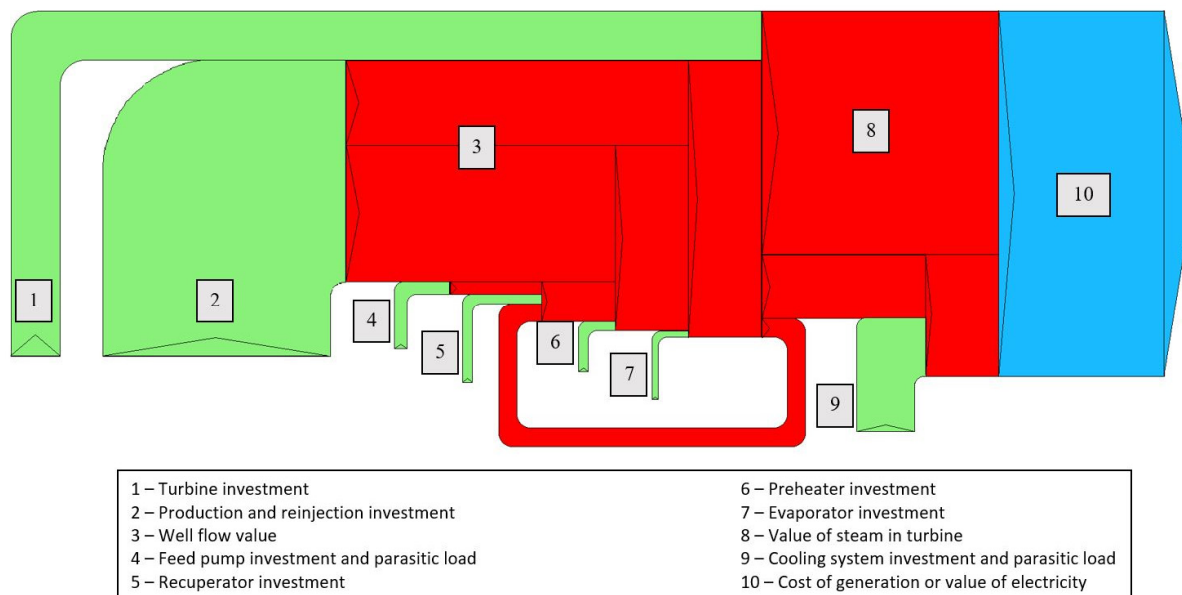


FIGURE 13: Value Flow diagram of the system

The Value Flow diagram shows the cost of exergy in the system. The length of the triangle on the side of a box represents the cost of exergy in each component. This diagram identifies the major source of cost in the system. The major contributor is the cost of production and reinjection, followed by the cooling system and its parasitic load, and the turbine investment. As described earlier on this section, the production and reinjection wells have the largest total investment and O&M cost rates in the system followed by the turbine but, when the parasitic load was considered, the cost rate in the cooling system becomes the second largest contributor.

The Value Flow diagram also shows that the minimum cost of generation is the sum of the cost of exergy in the stream in the turbine and the stream in the condenser which is equivalent to 132.17×10^{-3} USD/sec or 6.22 USDcents/kWh. This value represents the minimum cost of generating electricity of the system based on the cost balance. This cost only covers the cost of the power generating system, therefore, the real cost of generated electricity is expected to be higher as per the value determined using NPV analysis, 8.26 USDcents/kWh. Nevertheless, the minimum cost of generating electricity is much lower than the true cost of diesel in Mindoro that ranges from 18 to 74 USDcents/kWh or the existing subsidized approved generation rate of 11 USDcents/kWh.

The result for the cost of exergy is positive. Through evaluation of the Grassman diagram and the calculated thermoeconomics variables, the system could be further optimized. To do this, the components were arranged in descending order of the sum of cost of exergy destruction, investment and O&M cost rate (C_d+Z) (Table 13).

TABLE 13: Thermoeconomics variables

Component k	ϵ_k %	E_d kW	y_d %	C_d , USD/s	Z USD/s	C_d+Z USD/s	r_k %	f_k %
Turbine	84.31	1 839.00	10.12	16.32	17.62	33.94	18.60	61.57
Preheater	85.83	835.30	4.60	8.71	3.41	12.12	24.57	32.80
Condenser	85.60	519.00	2.86	0.00	9.29	9.29	43.36	72.87
Evaporator	83.29	2 053.00	11.29	6.56	2.14	8.69	28.46	29.50
Recuperator	74.91	277.60	1.53	3.37	3.44	6.80	102.80	67.41
Feed Pump	76.52	96.99	0.53	0.73	0.78	1.51	45.58	47.38

*The parameters used are defined in the nomenclature at the end of this report.

From the thermoeconomics viewpoint, the turbine and the preheater have the highest value of C_d+Z and are, therefore, the most important component of the system. The low value of exergetic efficiency f of the preheater and the evaporator shows that the cost associated with these components are comprised mostly of the exergy destruction. Thus, cost saving might be achieved by improving the components efficiency through the reduction of the exergy destruction even if the capital investment for this component will increase. However, as for the turbine and the feed pump, an improvement of the evaporator would not be possible as the quality of this component is based on the quality provided by the manufacturer. Therefore, cost saving can obtain through improvements in the preheater.

6. CONCLUSION

Power plant modelling and thermoeconomics modelling was used to determine the optimal capacity of the system, cost of development, minimum cost of generation, and exergetic evaluation.

The result of the modelling shows that the Montelago geothermal prospect could be capable of a generating 9390 kW electricity with a net generating capacity of 7650 kW. The system has thermal efficiency and exergetic efficiency of 5.92 and 43.55%, respectively. The obtained efficiencies are well within the range of 2.1 to 10.3% for thermal efficiency and 17.2 to 53.9% for exergetic efficiency.

Additionally, it was determined that the total cost of developing the prospect is 3574 USD/kW while the minimum cost of generation is 6.22 USDcents/kWh. However, this cost only covers the cost of the power generating system and does not cover the costs on offsite costs, indirect cost and other outlays, therefore, the real cost of generated electricity is expected to be higher than this value. That is why it is important to additionally analyse the system using the profitability evaluation. The profitability evaluation shows that the project starts to have a positive NPV when the tariff is higher than 8.21 USDcents/kWh with IRR of 10% which is the break-even point of the system. This is way lower than the current price of electricity available in the region which his 18 to 74 USDcents/kWh and still lower than the existing subsidized approved generation rate which is 11 USDcents/kWh.

Additionally, the exergetic analysis found that cost saving in the entire system might be achieved by improving the preheater's exergetic efficiency through the reduction of the exergy destruction even if the capital investment for this component will increase.

Therefore, it is concluded that, based on the described parameters, further developing the geothermal prospect is economical. However, it needs to be taken into consideration that as the prospect is further developed, new data might not be like the described parameters in this report. This means that the design considerations and constraints used in this report cannot be directly applied. Nevertheless, the study made on the Montelago geothermal prospect provided a wide overview using power plant and thermoeconomics modelling. Additionally, the model could be used as a base line for other authors who have an interest in conducting a similar study.

ACKNOWLEDGEMENTS

I want to express my sincerest gratitude to Lúdvík S. Georgsson, Ingimar Gudni Haraldsson and to the rest of the staff of the UNU-GTP for giving me the opportunity to be part of this training and for providing me with necessary support in the entire period of the program. Also, I would like to thank my advisers, Dr. Páll Valdimarsson and Dr. María Sigríður Guðjónsdóttir, for their guidance and supervision during the entire project period, and Lýður Skúlason for providing assistance and guidance with my report.

Also, I would like to thank my colleagues at the Philippines Department of Energy and the Mindoro Geothermal Power Corp. for providing me with all the necessary information and data that I needed to complete this report.

Lastly, I would also like to thank my family, the UNU Fellows of 2019 and my friends for their support.

This report would not have been possible without these people.

NOMENCLATURE

A	= Area (m ²).
C_k	= Cost of component (USD).
\dot{C}	= Cost of exergy (USD/s).
$c_{p,k}$	= Cost per exergy unit associated with fuel (USD/kJ).
c_k	= Cost per exergy unit (USD/kJ).
$c_{p,k}$	= Cost per exergy unit associated with product (USD/kJ).
$\dot{C}_{d,k}$	= Cost of exergy destruction (USD/s).
$\dot{C}_{e,k}$	= Cost of exergy stream exiting (USD/s).

\dot{C}_f	= Cost of exergy associated with fuel (USD/s).
$\dot{C}_{i,k}$	= Cost of exergy stream entering (USD/s).
$\dot{C}_{l,k}$	= Cost of exergy loss (USD/s).
$C_{l,O\&M}$	= Levelized cost of O&M (USD).
C_p	= Specific heat (kJ/kg-°C).
\dot{C}_p	= Cost of exergy associated with product (USD/s).
$\dot{C}_{q,k}$	= Cost of exergy stream heat transfer (USD/s).
$\dot{C}_{w,k}$	= Cost of exergy stream power (USD/s).
$CELF$	= Constant-escalation levelization factor.
CRF	= Cost recovery factor (%).
D	= Depth (feet).
\dot{e}_k	= Specific exergy rate of component (kJ/kg).
\dot{E}_k	= Exergy rate of component (kW).
$\dot{E}_{d,k}$	= Exergy rate of destruction of component (kW).
$\dot{E}_{f,k}$	= Exergy rate of component associated with fuel (kW).
$\dot{E}_{l,k}$	= Exergy rate of loss of component (kW).
$\dot{E}_{p,k}$	= Exergy rate of component associated with product (kW).
f_k	= Exergoeconomic factor (%).
h_0	= Enthalpy at the environment state (kJ/kg).
h_k	= Enthalpy (kJ/kg).
h_{s-5}	= Enthalpy exiting the turbine in ideal isentropic process (kJ/kg).
i_{eff}	= Nominal discount rate (%).
k	= Constant rate of change.
$LMTD$	= Logarithmic Mean Temperature Difference.
\dot{m}	= Mass flowrate (kg/s).
n	= Plant life (years).
p	= Pressure (bar).
PW_k	= Present worth cost of component (USD).
\dot{Q}	= Heat (Kw).
r_k	= Relative cost difference (%).
r_n	= Nominal escalation rate (in this report, this value was assumed to be 4%).
s_0	= Entropy at the environment state (kJ/kg-°C).
s	= Entropy (kJ/kg-°C).
S_k	= Salvage value (USD).
T_0	= Temperature at the environment state (°C).
T	= Temperature (°C).
U	= Overall heat transfer coefficient (kW/m ² -°C).
v	= Specific volume of fluid (m ³ /kg).
\dot{W}	= Gross power (kW).
\dot{W}_{net}	= Net power output (kW).
y_d	= Exergy destruction ratio (%).
y_l	= Exergy loss ratio (%).
\dot{Z}_k	= Sum of investment and O&M cost rates (USD/s).
\dot{Z}_k^{CI}	= Cost rate in capital investment of component (USD/s).
\dot{Z}_k^{OM}	= Cost rate in O&M of component (USD/s).
ΔP	= change in pressure (bar).
ϵ_k	= Exergetic efficiency (%).
η	= Efficiency (%).
τ	= Time of operations (seconds).

REFERENCES

- Adefila, S.S., Alam, M.M., Fagbenle R.O., and Oyedepo, S.O., 2015: Exergy costing analysis and performance evaluation of selected gas turbine power plants. *World J. Engineering*, 12-2, 161-176.
- Ahmed, S. J., 2019: *The Philippine energy transition: building a robust power market to attract investment, reduce prices, improve efficiency and reliability*. Institute for Energy Economics and Financial Analysis, report, 14 pp.
- Asmin, S.N., Catigtig, D., Pratama, A.B., Regandara, R., Saputra, M.P., and Suryantini, 2016: Geological, isothermal, and isobaric 3-D model construction in early stage of geothermal exploration. *Proceedings of the 5th ITB International Geothermal Workshop, Bandung, Indonesia*, 14 pp.
- Axelsson, G., and Halldórsdóttir, S., 2015: *Revised volumetric assessment of Montelago geothermal system*. ÍSOR – Iceland GeoSurvey, Reykjavík, report, ISOR-15020, 12 pp.
- Bejan, A., Moran, M., and Tsatsaronis, G., 1996: *Thermal design and optimization*. John Wiley & Sons, Inc., Canada, 533 pp.
- Clarke, J., 2014: *Optimal design of geothermal power plants*. Virginia Commonwealth University, Richmond, Virginia, 192 pp.
- Clemente, J. V., Alcober, H.C., de Guzman, R.C., and Bayrante, L.F., 2016: Country update on geothermal utilization and barriers affecting its growth – Philippines. *Proceedings of the 11th Asian Geothermal Symposium, Chiangmai, Thailand*, 6 pp.
- Climate-Data.org, 2019: *Climate data from Mindoro, Philippines*. Climate-Data.org, website: en.climate-data.org/asia/philippines/oriental-mindoro-1842/#temperature-graph.
- DOE, 2019a: 2018 Power statistics. Department of Energy, website: www.doe.gov.ph/sites/default/files/pdf/energy_statistics/03_2018_power_statistics_as_of_29_march_2019_generation_per_type.pdf.
- DOE, 2019b: *GEMD-NREP 2018-2040 report*. Department of Energy, Taguig, Philippines, unpublished internal report.
- DOE, 2019c: *Cost of geothermal exploration in the Philippines*. Department of Energy, Taguig, Philippines, unpublished internal report.
- DiPippo, R., 2016: *Geothermal power generation: developments and innovation*. Woodhead Publishing, Kidlington, UK, 822 pp.
- El-Eman, R.S., and Dincer, I., 2013: Exergy and exergoeconomic analyses and optimization of geothermal organic Rankine cycle. *Applied Thermal Engineering*, 59-1/2, 435-444.
- Fujii, H., Itoi, R., Jalilinasrabad, S., and Valdimarsson, P., 2011: Energy and exergy analysis of Sabalan binary geothermal power plant. *J. Geothermal Research Society of Japan*, 33-3, 113-121.
- GeothermEx, 2017: *Resource evaluation for the Montelago geothermal project, Oriental Mindoro, The Philippines*. GeothermEx, Richmond, CA, report, 89 pp.
- Hance, C.N., 2005: *Factors affecting costs of geothermal power development*. Geothermal Energy Association for the US Department of Energy, 64 pp.

Haraldsson, I.G., 2016: Efficiency in geothermal utilization processes. Presented at “SDG Short Course I on Sustainability and Environmental Management of Geothermal Resource Utilization and the Role of Geothermal in Combating Climate Change”, organized by UNU-GTP and LaGeo, in Santa Tecla, El Salvador, 66 pp.

IFC, 2013: *Success of geothermal wells: a global study*. International Finance Corporation, World Bank Group, Washington, DC, 76 pp.

Jing, D., Liu, P., Tian, H., Shu, G., and Wang, X., 2017: Operational profile based thermal-economic analysis on an organic Rankine cycle using for harvesting marine engine’s exhaust waste heat. *Energy Conversion and Management*, 2017, 107-123 pp.

Kotas, T.J., 1985; *The exergy method of thermal plant analysis*. Anchor Brendon Ltd, Tiptree, Essex, Great Britain, 296 pp.

Lemmens, S., 2016: Cost of engineering techniques and their applicability for cost estimation of organic Rankine cycle systems. *Energies*, 9-7, 18 pp.

Lukawski, M., 2009: *Design and optimization of standardized organic Rankine cycle power plant for European conditions*. The School for Renewable Energy Science, Akureyri, Iceland, 76 pp.

NGCP, 2019: *Transmission development plan 2016-2040 final report volume 1: major network development*. NGCP.ph, website: www.ngcp.ph/Attachment-Uploads/TDP%202016-2040%20Final%20Report%20Volume%201%20Major%20Network%20Development-2019-05-14-16-43-41.pdf

SKM, 2011: *Assessment of the Montelago prospect, Philippines*. Green Earth Energy Ltd, report, 38 pp.

Thórhallsson, S., 2005: Common problems faced in geothermal generation and how to deal with them. Presented at “Workshop for Decision Makers on Geothermal Projects and Management”, organized by UNU-GTP and KenGen, Naivasha, Kenya, 12 pp.

Valdimarsson, P., 2010: Production of electricity from a geothermal source. In: *Geothermal energy*, Macedonian Geothermal Association, Skopje, Macedonia, 50-180.

van Leeuwen, W.A., 2016: The Montelago geothermal prospect. In: *Geothermal exploration using the magnetotelluric method*. Utrecht University, Dept. of Earth Sciences, the Netherlands, 133-194.

Wikipedia.org, 2019: *Mindoro, Philippines*. Wikipedia, website: en.wikipedia.org/wiki/Mindoro.

XE Corporation, 2019: *XE currency converter*, website: www.xe.com/currencyconverter/convert/?Amount=1&From=PHP&To=USD.

APPENDIX I: List of geothermal areas with low- to intermediate-temperature geothermal resources (Department of Energy, 2019b)

No.	Region	Project name	Location	Classification based on temp.	Capacity (MW)
1	I	Cervantes	Ilocos Sur	Intermediate-temp. system	TBD
2	III	Negron-Cuadrado	Zambales/Pampanga	Intermediate-temp. system	TBD
3	IV-A	San Juan	Batangas	Intermediate-temp. system	20
4	IV-A	Mabini	Batangas	Intermediate-temp. system	20
5	IV-A	Maricaban Island	Batangas	Intermediate-temp. system	TBD
6	IV-A	Puting-Lupa	Laguna	Intermediate-temp. system	TBD
7	IV-A	Tayabas-Lucban	Tayabas/Quezon	Intermediate-temp. system	TBD
8	IV-A	Tiaong	Laguna/Quezon/ Batangas	Intermediate-temp. system	TBD
9	IV-B	Montelago	Oriental Mindoro	Intermediate-temp. system	40
10	V	Southern Bikol	Sorsogon	Intermediate-temp. system	40
11	VIII	Bato Lunas	Leyte	Intermediate-temp. system	65
12	IX	Lakewood	Zamboanga del Sur	Intermediate-temp. system	40
13	X	Sapad-Salvador	Lanao del Norte	Intermediate-temp. system	30
14	X	Ampiro	Misamis Occidental	Intermediate-temp. system	30
15	XI	Mt. Parker	South Cotabato	Intermediate-temp. system	60
16	XI	Balut Island	Davao Occidental	Intermediate-temp. system	23
17	XII	Mt. Zion	North Cotabato	Intermediate-temp. system	TBD
18	XIII	Mainit	Surigao del Norte	Intermediate-temp. system	30
19	CAR	Buguias-Tinoc	Ifugao	Intermediate-temp. system	60
20	CAR	Sal-lapadan-Boliney-Bucloc-Tubo	Abra	Low-temperature system	TBD*

*TBD – to be determined

APPENDIX II: Major component cost estimates in the power plant, in USD

	El-Eman & Dincer (2013)	Lemmens (2016)	Jing, et al. (2017)	(Páll Valdimarsson, pers. comm., 2019)
Condenser	1 078 000	2 588 000	191 000	1 979 000
Evaporator	544 000	544 000	103 000	455 000
Feed Pump	38 000	38 000	340 000	165 000
Preheater	814 000	814 000	148 000	727 000
Recuperator	819 000	819 000	149 000	732 000
Turbine-Generator				3 756 000
Turbine	249 000	591 000	429 000	
Generator		1 747 000		
Total Cost	3 544 000	7 142 000	1 361 000	7 815 000